

Hypoxic-Ischaemic Encephalopathy Prognosis using Susceptibility Weighted Image Analysis based on Histogram Orientation Gradient

Zhen Tang¹^a, Sasan Mahmoodi¹, Angela Darekar² and Brigitte Vollmer³

¹*School of Electronics and Computer Science, University of Southampton, Southampton SO17 1BJ, U.K.*

²*Department of Medical Physics, University Hospital Southampton NHS Foundation Trust, Southampton SO16 6YD, U.K.*

³*Clinical Neurosciences and Clinical and Experimental Sciences, Faculty of Medicine, University of Southampton, SO17 1BJ, U.K.*

Keywords: Hypoxic-Ischaemic Encephalopathy, Susceptibility-weighted Imaging, HOG, Motor, Cognitive Outcomes.

Abstract: The aim of this study is to analyse the susceptibility-weighted magnetic resonance images (SWI) by using Histogram of Oriented Gradients (HOG) as a global feature to identify areas of the neonatal brain affected by Hypoxic-ischaemic encephalopathy (HIE). 42 infants with neonatal HIE have undergone under SW imaging in the neonatal period and have been investigated through neurodevelopmental assessment at 24 months of age. HOG features are used to represent the whole brain SW images and the region of interest separated from the brain image registration algorithm. We use k-nearest neighbours (*kNN*) and random forest to classify the SWI images into normal and abnormal groups, and then we compare our results to our previous work. The result shows an effective classification, which achieved an accuracy of 76.25 ± 10.9 . Our research suggests that automated analysis of neonatal SWI images can identify brain regions affected by HIE on SWI images and predict motor and cognitive outcomes.

1 INTRODUCTION

Hypoxic-ischaemic (HI) is a type of neonatal brain damage caused by oxygen deprivation and limited blood flow, and it is an important cause of perinatal death or neurodevelopmental (motor, cognitive, behavioural and speech impairments) impairment in newborns worldwide (Nadeem et al., 2011; Massaro et al., 2015). Due to the complexity of neonatal brain damaged by HI, traditional methods of diagnosing hypoxic-ischaemic encephalopathy (HIE) results are time-consuming and inefficient (Macleod et al., 2020). Therefore, the application of an automatic method will be useful to streamline the procedure for specialists to diagnose an early diagnosis.

Magnetic resonance imaging (MRI) has become the standard for the assessment and study of neonatal HI injury and developmental abnormalities (Midiri et al., 2021). Susceptibility weighted image (SWI) is increasingly used in clinical practice because of its sensitivity to haemorrhage and calcification (Mittal et al., 2009; Sehgal et al., 2005). SWI images of infants with HIE may be useful biomarkers for diagnosis and

outcome prediction (Zhang et al., 2019). Quantitative analysis of deep medullary venous structures in SWI images were used to assess the severity of HI injury (Kim et al., 2020), and the first-order texture parameters derived from SWI were employed to distinguish between infants with HIE and infants without HIE. An approach (Li et al., 2019) combined the SWI images and magnetic resonance spectroscopy (MRS) for early diagnosis in infants with HIE. Another approach of automatic detection for infants injured by HI was offered (Wu et al., 2017), and the Hessian eigenvalue of the vessels in SWI images was applied to classify the 48 infants with HIE and 10 infants without HIE based on a scoring system suggested by Kitamura (Kitamura et al., 2011). In (Citraro et al., 2017), they developed an extended 3D local binary pattern to distinguish the images of a three-dimensional SWI dataset of infants with HIE based on their oxygenation status. In our previous work (Tang et al., 2020), balanced datasets of SWI images of newborns with HIE and the neurological outcomes of these infants at age 24 months were used for classification, as well as the

 <https://orcid.org/0000-0002-9154-5182>

motor and cognitive outcomes for regression analysis. From the above study, we see that there are two major issues in SWI analysis in the context of neonatal HIE: (a) unbalanced data and (b) segmentation and extraction of different brain regions.

In the present paper, we propose an automatic framework to detect neonatal hypoxic-ischaemic brain injury by extracting the HOG features of the brain and vessels in SWI images to analyse SWIs of HIE infants. Then, an image registration technique (Avants et al., 2009) is used to identify the brain regions by matching the SWIs with a brain template. The HOG is utilised to extract features of these brain regions. All extracted feature vectors as the input are fed into *kNN* and random forest algorithms for classification of HIE infants with developmental outcome at age 24 months.

2 DATA ACQUISITION

This use of anonymised, routinely collected clinical data have been granted an ethical approval from the Health Research Authority (HRA), Health and Care Research Wales (IRAS ID 279072; REC reference 20/HRA/0260), and the National Research Ethics Service London, City & East (IRAS ID 143392; REC reference 13/LO/1948).

3 METHODS

In this study, 42 infants with neonatal HIE born at gestational age $>36+6$ weeks who underwent hypothermia treatment were scanned using a 1.5T Siemens Symphony MRI scanner. The scan included proton density, T1-weighted, T2-weighted, turbo inversion recovery and SWI. SWI data was acquired using a flow-compensated, spoiled gradient echo (FLASH) sequence, with the following pulse sequence parameters: TR/TE/flip angle = 50 ms/40 ms/12°, voxel size = $0.9 \times 0.9 \times 2$ mm³, bandwidth = 70 Hz/pixels.

The participants in this study were scanned at a mean age of 7.8 days (min 1 day, max 34 days) after birth. Assessment of cognitive, motor, and language development with the Bayley Scales of Infant and Toddler Development 3 (Bayley-3; Edmonds et al., 2020) were done at age 24 months.

The composite scores calculated from Bayley-3, a standardised tool used to assess neurodevelopment, including cognitive, language and motor of infants aged from 1–42 months (Edmonds et al., 2020), are

used. Bayley-3 composite scores have a mean of 100 and a standard deviation (SD) of 15. In the case of a Bayley-3 composite score within less than one SD of the mean (>85), development is considered age-appropriate; mild delay based on a composite score greater than 1–1.5 SD below the mean (77.5–85), and moderate or severe delays if the score is more than 1.5 SD below the mean (<77.5). In our research, the focus is on cognitive and motor development. Bayley-3 outcome data could be obtained for 29 children on the cognitive scale and 28 children on the motor scale (some children were unable to complete the motor tasks because of impaired motor function).

3.1 Image Processing

We applied an active contour model (Kass et al., 1988) for the brain segmentation to remove the skull, eyes and the background from the SWI images to reduce the noise in the images as shown in Figure 1(b).

3.2 Feature Extraction of HOG

This section must be in one column. As SWI images can sensitively capture the blood vessels and vascular structures in the brain (Reichenbach, 2020), we employ the Histogram of Oriented Gradients (HOG) feature descriptors for object detection (Dalal and Triggs, 2005). HOG is a powerful feature extraction technique that calculates the occurrences of gradient orientation in local parts of an image. Before proceeding with the calculation of HOG feature vectors, we crop the SWI images into an image of 110×130 pixels (110 pixels width and 130 pixels height) to avoid the effect of redundant HOG features from the background in SWI images, as shown in Figure 1. Then, the first step of HOG is to calculate the gradient of each pixel. We denote $I(x, y)$ to be the SWI image and use a Sobel kernel of size (3×3) to obtain the horizontal and vertical gradients of each pixel. The gradient is composed of magnitude and angle from SWI image using following formulae:

$$M(x, y) = \sqrt{G_x^2 + G_y^2} \quad (1)$$

$$\theta = \text{Arctan} \frac{G_y}{G_x} \quad (2)$$

Here, G_x and G_y are the gradients of each pixel in x and y direction. $M(x, y)$ denotes the magnitude and θ denotes gradient direction for the pixel. After obtaining the gradient (including magnitude and direction) of each pixel, the cropped SWI images are

divided into 10×10 pixels to form a cell. For each cell, a histogram with four bins and an angle range of 45 degrees is developed. Finally, one cell is formed into a block. The histogram vector and the normalization process can be calculated as follows:

$$v = \{b_1, b_2, \dots, b_i\} \quad (3)$$

$$v' = v / \sqrt{\|v\|_2^2 + \varepsilon^2} \quad (4)$$

where b is the value of each bin, ε is a small positive value used for regularization to avoid division by zero.

For each SWI image of each infant with HIE, the total length of HOG features is $4 \times 11 \times 13 = 572$. We sum up the HOG features of each SWI image belonging to the same infant with neonatal HIE to create a feature vector, V_{whole} , describing the image, and then the feature vector for each infant is normalised. Figure 1 shows HOG of SWI image with HIE.

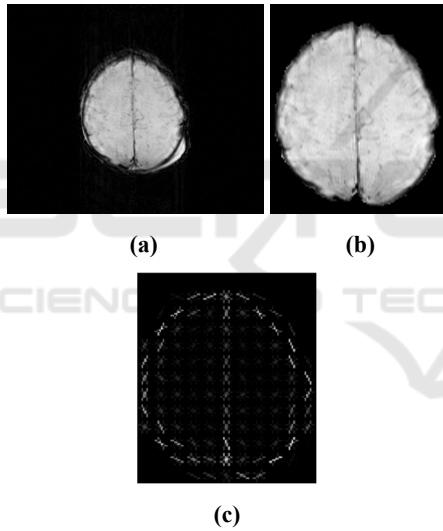


Figure 1: (a) Original SWI image (b) Cropped image after active contour (c) HOG image.

3.3 Image Registration

In order to look for the brain regions affected by hypoxic-ischaemic, we register the atlas, including the average intensity image, the tissue density maps, the structure density maps, and the maximum probabilistic maps and labels, as a reference template with the SWIs to identify individual lobes in SWIs. The brain template, LPBA40/AIR, (<https://resource.loni.usc.edu/resources/atlas-downloads/>) is selected for this study. The image registration of SWI datasets is carried out using Advanced Normalisation Tools (ANTs) (Avants et al., 2009),

which has the best quality for registration of brain magnetic resonance images. We convert all SWI images of each infant in our dataset into 3D brain images to be registered. The strategy on ANTs registration programme for which we opt for, is to map the SWI images to the template brain images using similarity transform and obtain the registered SWI images.

The LPB40/AIR template provides a standard normalised space containing 56 brain structures and partition labels, such as frontal lobe and parietal lobe (Shattuck et al., 2008). Since SWI images of each infant with neonatal HIE are transformed/registered into a template brain of an atlas based on an image registration method, we map the 56 labels of the maximum probabilistic maps onto the new registered SWI images for analysis. We eventually consider the primary motor area, premotor area, and supplementary motor area of 3D images to explore the relationship between the SWI features in these areas and motor outcomes at 24 months of age. To explore the relationship with cognitive outcomes frontal lobe, parietal lobe and temporal lobe of the brain as a 3D brain were examined. As shown in Figure 2(b), the area covered in blue represents the motor area. The motor areas of the brain in SWI images are therefore selected by registering SWI images to the template brain and the motor areas are left in the 3D image with the rest of the brain being ignored (i.e. set to zero).

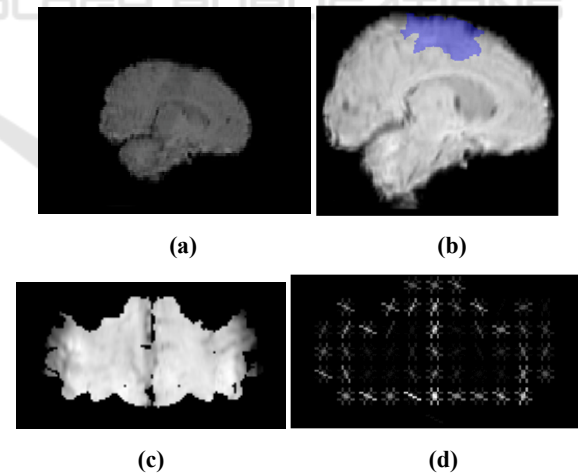


Figure 2: (a) Original brain image. (b) Brain image after registration and motor area covered by blue (c) 2D image of motor area (d) HOG of motor area.

Finally we consider the 3D motor region images as slices and compute HOG feature vector V_{motor} associated with the motor region. In a similar fashion, we select frontal, parietal and temporal lobes for

cognitive regions of the brain by using the aforementioned registration method. Then by only considering these three lobes on the 3D SWIs and ignoring the rest of the brain, we measure the HOG feature vectors V_{lobes} associated with these three lobes.

4 RESULT

4.1 Classification for Motor Outcome

For the 28 infants with HIE who were assessed with Bayley-3 scales, 25 infants have normal motor development (scores >85), two infants have mild motor delay (scores between 77.5–85), and one has severe motor delay (score <77.5). The normal group with normal motor outcomes and the abnormal group with mild motor delays and severe motor delays are used as two classes for classification.

We employ HOG feature vectors V_{whole} and V_{motor} for each infant of two classes as training data. kNN and RF classifications are performed based on these feature vectors.

Likewise, balanced data based on three infants with delayed motor scores and three infants with normal motor scores randomly selected from a group of 25 infants with normal motor scores has been used for classification. By repeating the above process ten times with random selections from normal group, the mean and standard deviation of classification accuracies are calculated. Leave-one-out strategy is employed here, and final accuracy is reported in Table 1.

4.2 Classification for Cognitive Outcome

29 infants, of which 25 have normal cognitive outcome (scores >85), three had mild cognitive delay (scores between 77.5–85) and one had severe cognitive delay (scores <77.5), are partitioned by two groups: the normal group with normal cognitive outcomes and the abnormal group with mild and severe cognitive delay outcomes. Here, we use HOG feature vectors V_{whole} and V_{lobes} for each infant with cognitive outcome as an input of kNN and RF classifications.

Again, we utilise the balanced data, in which four infants with delayed cognitive scores and four infants with normal cognitive scores were randomly selected from the 25 infants in the normal cognitive score group to measure the performance of kNN and RF classification with a leave-one-out strategy. By

repeating ten times the aforementioned classification, the mean and standard deviation of final accuracy is computed in Table 1.

4.3 Experimental Result

The classification analysis based on the motor outcome and cognitive outcome of infants with HIE all are a two class tasks: normal group and abnormal group. HOG feature vectors from whole brain V_{whole} and from different functional areas, including motor area V_{motor} and cognitive regions of the brain V_{lobes} , are fed to kNN and RF classification for comparison. All classification performances are compared to our previous work (Tang et al., 2020), which means we extract features from motor area and frontal, temporal and parietal lobes by using the method (Tang et al., 2020) to classify.

Table 1: Classification performance comparison.

	Features	kNN	RF
Motor outcome			
Whole brain	Tang et al., 2020	48.33±9.46	69.91±18.92
	V_{whole}	55.01±8.05	63.33±7.03
Motor area	Tang et al., 2020	41.52±16.14	68.83±14.59
	V_{motor}	61.67±15.81	71.67±11.24
Cognitive outcome			
Whole brain	Tang et al., 2020	53.75±15.64	61.25±13.75
	V_{whole}	53.75±13.24	70.00±6.45
Frontal+temporal+parietal lobes	Tang et al., 2020	56.25±13.5	62.5±10.2
	V_{lobes}	57.5±8.74	76.25±10.9

Table 1 shows the different classification results using features from different strategies. For motor development outcome, features from (Tang et al., 2020) still produce better accuracy than HOG features represented by vector V_{whole} in whole brain area. But in the motor area of the brain, the classification performance of feature vector V_{motor} using HOG feature descriptor exceeds that of features in (Tang et al., 2020). Compared with methods (Tang et al., 2020), HOG features we propose in this paper perform higher accuracy in both whole brain area and motor area of the brain for cognitive outcome. From Table 1, HOG features obtained from only the motor areas show better classification accuracies for HIE motor development outcome prognosis in SWI

images. Also the feature vectors generated by HOG descriptors in frontal, parietal and temporal lobes for cognitive regions of the brain are effective in classifying infants with cognitive outcome in SWI images.

Figure 3 shows the inter/intra- class variations for two normal and abnormal groups for motor outcome

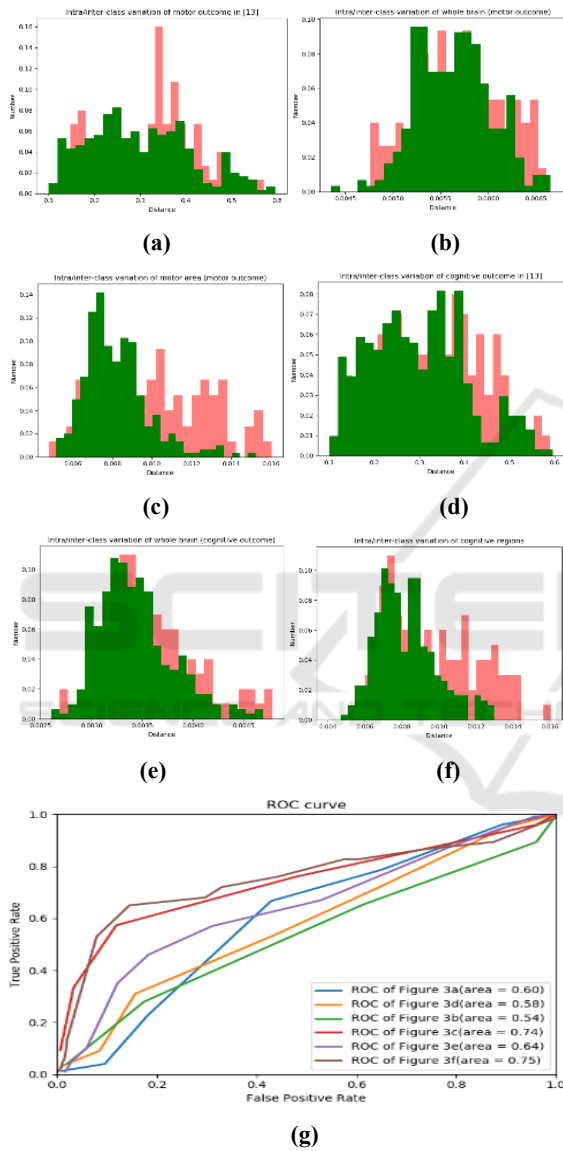


Figure 3: Inter/intra-class variations associated with motor outcome for: (a) features obtained from (Tang et al., 2020); (b) HOG features of whole brain with motor outcome; (c) HOG features of motor area. Inter/intra-class variations associated with cognitive outcome for: (d) features obtained from (Tang et al., 2020); (e) HOG features of whole brain with cognitive outcome; (f) HOG features of cognitive regions. (g) ROC curves of above inter/intra- class variations plots.

(Figure 3(a, b and c)), and cognitive outcome (Figure 3(d, e and f)). The green histograms represents the intra-class variation for infants in the same group and the red histograms show the inter-class for infants from two different groups. Histograms of features extracted using methods in (Tang et al., 2020) (figure 3(a and d)) and using methods in this paper (figure 3(b, c, e, and f)) are normalised to the area below each histogram. As shown in figure 3(a and d), the two histograms are highly overlapped. Figure 3(b) presents the inter- and intra- class variation histograms of HOG feature vectors from whole brain area between normal and abnormal groups in infants with motor outcome, and furthermore figure 3(c) shows the inter- and intra-class variations of HOG features from motor area of brain. Figure 3(e) shows the inter/intra-class variation histograms of HOG features from whole brain area between normal and abnormal groups in infants with cognitive outcome, while figure 3(f) shows the variations of HOG features from cognitive regions. The Receiver Operator Characteristic (ROC) curves corresponding to the inter- and intra- class variations are shown in figure 3(g). As observed from figure 3(c and f), the overlap between two histograms and the areas under the ROC curves (brown and red curves) illustrate a better performance after using image registration to extract the HOG features of motor areas and cognitive areas.

5 CONCLUSIONS

In this paper, a HOG feature extraction method for detection of neonatal hypoxic-ischaemic brain injury in SWI images has been used. We design a HOG feature descriptor to gain feature vectors to classify HIE SWI images along with *kNN* and random forest classifiers into normal and abnormal groups based on motor and cognitive assessments of infants with HIE at age 24 months. In addition, we map our SWI images to a brain template containing different function regions by an image registration algorithm to obtain motor and cognitive regions of the brain. Then HOG feature vectors of motor and cognitive regions are used for classification to help us identify which areas of the brain are responsible for abnormal outcome. Compared to our previous work (Tang et al., 2020), we achieve outstanding performance in the classification experimentations on HIE infants with regards to motor development outcome by using HOG features of motor areas of the brain in SWI images, 71.67 ± 11.24 , and similarly HOG features of frontal, temporal and parietal lobes of the brain show

better classification performance for cognitive outcome, 76.25 ± 10.9 . In the future, we plan to explore the relationship between other regions of the brain and assessment outcome at two years of age. One interesting future work is to combine our previous method (Tang et al., 2020) with the method presented in this paper to improve the performance of our system.

REFERENCES

- Nadeem, M., Murray, D. M., Boylan, G. B., Dempsey, E. M., & Ryan, C. A. (2011). Early blood glucose profile and neurodevelopmental outcome at two years in neonatal hypoxic-ischaemic encephalopathy. *BMC Pediatrics*, 11(1), 1–6.
- Massaro, A. N., Evangelou, I., Fatemi, A., Vezina, G., Mccarter, R., Glass, P., & Limperopoulos, C. (2015). White matter tract integrity and developmental outcome in newborn infants with hypoxic - ischemic encephalopathy treated with hypothermia. *Developmental Medicine & Child Neurology*, 57(5), 441–448.
- Mittal, S., Wu, Z., Neelavalli, J., & Haacke, E. M. (2009). Susceptibility-weighted imaging: Technical aspects and clinical applications, part 2. *American Journal of Neuroradiology*, 30(2), 232–252.
- Sehgal, V., Delproposito, Z., Haacke, E. M., Tong, K. A., Wycliffe, N., Kido, D. K., & Reichenbach, J. R. (2005). Clinical applications of neuroimaging with susceptibility-weighted imaging. *Journal of Magnetic Resonance Imaging: An Official Journal of the International Society for Magnetic Resonance in Medicine*, 22(4), 439–450.
- Macleod, R., O’Muircheartaigh, J., Edwards, A. D., Carmichael, D., Rutherford, M., & Counsell, S. J. (2020). Automatic Detection of Neonatal Brain Injury on MRI. In *Medical Ultrasound, and Preterm, Perinatal and Paediatric Image Analysis* (pp. 324–333). Springer, Cham.
- Midiri, F., La Spina, C., Alongi, A., Vernuccio, F., Longo, M., Argo, A., & Midiri, M. (2021). Ischemic hypoxic encephalopathy: The role of MRI of neonatal injury and medico-legal implication. *Forensic Science International*, 110968.
- Zhang, X., Zhang, Y., & Hu, Q. (2019). Deep learning based vein segmentation from susceptibility-weighted images. *Computing*, 101(6), 637–652.
- Kim, H. G., Choi, J. W., Han, M., Lee, J. H., & Lee, H. S. (2020). Texture analysis of deep medullary veins on susceptibility-weighted imaging in infants: Evaluating developmental and ischemic changes. *European Radiology*, 30(5), 2594–2603.
- Li, X., Zhang, W., Liu, D., & Zeng, Y. W. (2019). Effect of 3.0 T magnetic resonance SWI and MRS on early diagnosis of neonatal HIE and regression analysis of related predictive factors. *Journal of Hainan Medical University*, 25(1), 75–78.
- Wu, S., Mahmoodi, S., Darekar, A., Vollmer, B., Lewis, E., & Liljeroth, M. (2017, July). Feature extraction and classification to diagnose hypoxic-ischemic encephalopathy patients by using susceptibility-weighted MRI images. In *Annual Conference on Medical Image Understanding and Analysis* (pp. 527–536). Springer, Cham.
- Kitamura, G., Kido, D., Wycliffe, N., Jacobson, J. P., Oyoyo, U., & Ashwal, S. (2011). Hypoxic-ischemic injury: Utility of susceptibility-weighted imaging. *Pediatric Neurology*, 45(4), 220–224.
- Citraro, L., Mahmoodi, S., Darekar, A., & Vollmer, B. (2017). Extended three-dimensional rotation invariant local binary patterns. *Image and Vision Computing*, 62, 8–18.
- Tang, Z., Mahmoodi, S., Dasmahapatra, S., Darekar, A., & Vollmer, B. (2020, July). Ridge detection and analysis of susceptibility-weighted magnetic resonance imaging in neonatal hypoxic-ischaemic encephalopathy. In *Annual Conference on Medical Image Understanding and Analysis* (pp. 307–318). Springer, Cham.
- Edmonds, C. J., Helps, S. K., Hart, D., Zatorska, A., Gupta, N., Cianfaglione, R., & Vollmer, B. (2020). Minor neurological signs and behavioural function at age 2 years in neonatal hypoxic ischaemic encephalopathy (HIE). *European Journal of Paediatric Neurology*, 27, 78–85.
- Kass, M., Witkin, A., & Terzopoulos, D. (1988). Snakes: Active contour models. *International Journal of Computer Vision*, 1(4), 321–331.
- Reichenbach, J. R. (2020). Susceptibility weighted imaging. In *Neuroimaging Techniques in Clinical Practice* (pp. 165–187). Springer, Cham.
- Dalal, N., & Triggs, B. (2005, June). Histograms of oriented gradients for human detection. In *2005 IEEE Computer Society Conference on Computer Vision and Pattern Recognition (CVPR’05)* (Vol. 1, pp. 886–893). IEEE.
- Avants, B. B., Tustison, N., & Song, G. (2009). Advanced normalization tools (ANTS). *Insight j*, 2(365), 1–35.
- Shattuck, D. W., Mirza, M., Adisetiyo, V., Hojatkashani, C., Salamon, G., Narr, K. L., & Toga, A. W. (2008). Construction of a 3D probabilistic atlas of human cortical structures. *Neuroimage*, 39(3), 1064–1080.